

# Theoretical status of $\epsilon'/\epsilon$ \*

Ulrich Nierste

Fermilab Theory Division, MS106, Batavia IL60510, USA

I give a detailed introduction into the theoretical formalism for  $\epsilon'/\epsilon$ , which measures direct CP-violation in  $K \rightarrow \pi\pi$  decays. The current status of hadronic matrix elements and the strange quark mass is discussed. Several possible explanations of the unexpectedly high experimental results for  $\epsilon'/\epsilon$  are pointed out: A small strange quark mass, an enhancement of the hadronic parameter  $B_6^{(1/2)}$  from the  $\sigma$  resonance, an underestimate of isospin breaking and possible new physics contributions in the  $\bar{s}dZ$ -vertex and the  $\bar{s}d$ -gluon-vertex.

## 1. Setting the scene

This year has surprised us with new experimental results for  $\epsilon'/\epsilon$ , which measures direct CP-violation in  $K \rightarrow \pi\pi$  decays. Until February 1999 the experimental situation was inconclusive: While the CERN NA31 [1] experiment has clearly shown a non-vanishing  $\epsilon'/\epsilon$ , the Fermilab E731 result [2] was consistent with zero. With the new measurements of the Fermilab KTeV [3] and the CERN NA48 [4] collaborations this issue is settled now in favour of the non-zero NA31 result. The new world average reads

$$\text{Re} \frac{\epsilon'}{\epsilon} = (21.1 \pm 4.6) \cdot 10^{-4}. \quad (1)$$

The establishment of direct CP-violation rules out old superweak models. Yet while the Standard Model predicts a non-vanishing  $\epsilon'/\epsilon$ , the value in (1) came as a surprise to many theorists, as it exceeds most theoretical predictions. In the following I will try to illuminate the possible sources of this discrepancy.

The flavour eigenstates of neutral K mesons,

$$|K^0\rangle \sim \bar{s}d \quad \text{and} \quad |\bar{K}^0\rangle \sim s\bar{d},$$

combine into mass eigenstates  $|K_L\rangle$  and  $|K_S\rangle$  due to  $K^0-\bar{K}^0$  mixing depicted in Fig. 1. CP-violation in neutral Kaon decay is illustrated in Fig. 3.  $|K_L\rangle$  and  $|K_S\rangle$  are not CP eigenstates, because the  $\Delta S = 2$  amplitude inducing  $K^0-\bar{K}^0$  mixing violates CP. This *indirect CP-violation* has been discovered in 1964 by Christenson, Cronin, Fitch and Turlay [5]. By contrast *direct CP-violation* denotes CP-violation in the  $\Delta S = 1$  amplitude triggering the decay. It allows a CP-odd initial state to decay into a CP-even final state and vice versa. The dominant contributions to direct CP-violation in the Standard Model are depicted in Fig. 2.

\*Invited plenary talk at QCD 99, July 7-13th 1999, Montpellier, France

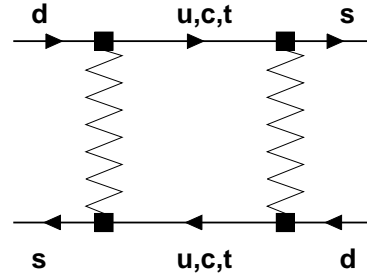


Figure 1. Standard Model  $\Delta S = 2$  box diagram. The zigzag lines denote W-bosons.

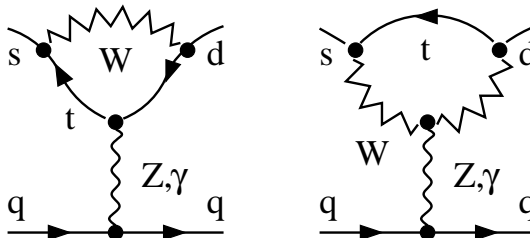
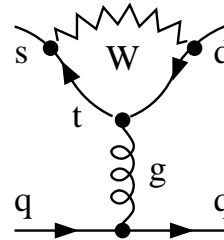


Figure 2. The  $\Delta S = 1$  diagrams dominating  $\epsilon'$  in the Standard Model: QCD and electroweak penguin diagrams.

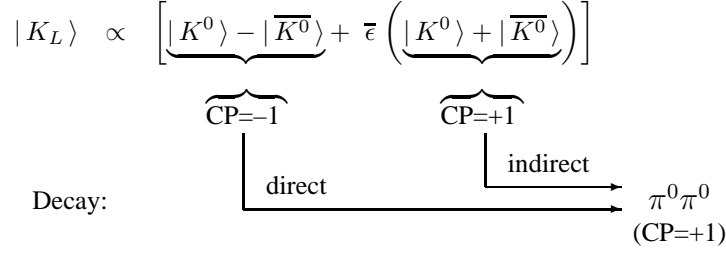


Figure 3. Direct and indirect CP-violation in  $K_L$  decay. The pattern for  $K_S$  decay is analogous.

In order to disentangle and quantify the two types of CP-violation one introduces isospin amplitudes:

$$\begin{aligned}\mathcal{A}(K^0 \rightarrow \pi^0\pi^0) &= \sqrt{\frac{2}{3}}A_0e^{i\delta_0} - \sqrt{\frac{4}{3}}A_2e^{i\delta_2} \\ \mathcal{A}(K^0 \rightarrow \pi^+\pi^-) &= \sqrt{\frac{2}{3}}A_0e^{i\delta_0} + \sqrt{\frac{1}{3}}A_2e^{i\delta_2} \\ \mathcal{A}(K^+ \rightarrow \pi^+\pi^0) &= \sqrt{\frac{3}{2}}A_2e^{i\delta_2}.\end{aligned}\quad (2)$$

In the limit of exact isospin symmetry, the hadronic final state interaction only produces non-vanishing strong phases  $\delta_0$  and  $\delta_2$  of the isospin  $I = 0$  and  $I = 2$  amplitudes in (2). Rescattering between the  $(\pi\pi)_{I=0}$  and  $(\pi\pi)_{I=2}$  state stems only from small isospin breaking effects, which will appear as a correction term in the formula for  $\epsilon'$ . The isospin amplitudes  $A_0$  and  $A_2$  are still complex, they contain the information on the CP-violating weak phases. For the CP-conjugated amplitudes to (2) describing  $\bar{K}^0$  and  $K^-$  decay one needs to replace  $A_0$  and  $A_2$  in (2) by their complex conjugates without changing the strong phases  $\delta_0$  and  $\delta_2$ . In phenomenological analyses of  $\epsilon'$  one takes the real parts of  $A_0$  and  $A_2$  from experiment:

$$\begin{aligned}\text{Re } A_0 &= 3.33 \cdot 10^{-7} \text{ GeV} \\ \omega &= \frac{\text{Re } A_2}{\text{Re } A_0} = \frac{1}{22.2}.\end{aligned}\quad (3)$$

The smallness of  $\omega$  has motivated the phrase “ $\Delta I = 1/2$  rule”, because isospin changes by a half unit in the dominant  $K \rightarrow (\pi\pi)_{I=0}$  decay.

Direct CP-violation requires the interference of at least two amplitudes with different strong (and weak)

phases. Hence

$$\begin{aligned}\epsilon &= \frac{\mathcal{A}(K_L \rightarrow (\pi\pi)_{I=0})}{\mathcal{A}(K_S \rightarrow (\pi\pi)_{I=0})} \\ &= (2.280 \pm 0.013) \cdot 10^{-3} e^{i\pi/4}\end{aligned}\quad (4)$$

purely measures indirect CP-violation. Direct CP-violation is encoded in  $\epsilon'$  with

$$\begin{aligned}\frac{\epsilon'}{\epsilon} &= \frac{1}{\sqrt{2}} \left[ \frac{\mathcal{A}(K_L \rightarrow (\pi\pi)_{I=2})}{\mathcal{A}(K_L \rightarrow (\pi\pi)_{I=0})} - \frac{\mathcal{A}(K_S \rightarrow (\pi\pi)_{I=2})}{\mathcal{A}(K_S \rightarrow (\pi\pi)_{I=0})} \right] \\ &= \frac{1}{\sqrt{2}|\epsilon|} \text{Im} \left( \frac{A_2}{A_0} \right) \\ &= \frac{\omega}{\sqrt{2}|\epsilon|} \left[ \frac{\text{Im } A_2}{\text{Re } A_2} - \frac{\text{Im } A_0}{\text{Re } A_0} \right].\end{aligned}\quad (5)$$

The phase of  $\epsilon'$  is  $\pi/2 + \delta_2 - \delta_0$  and numerically coincides with the phase of  $\epsilon$ .

The Standard Model predicts both indirect and direct CP-violation. The necessary CP-violating phases originate from the elements  $V_{u_i d_j}$  of the Cabibbo-Kobayashi-Maskawa (CKM) matrix. They enter the diagrams in Figs. 1 and 2 at the couplings of the W-boson to the quarks. The single complex phase  $\gamma$  in the CKM matrix must fit all CP-violating observables in  $K$ - and  $B$ -physics and moreover is also constrained by CP-conserving quantities. This will be a litmus test for the standard model and eventually open the door to new physics, once the dedicated B-physics experiments at  $e^+e^-$  [6] and hadron colliders [7] deliver data and the rare Kaon decays  $K^+ \rightarrow \pi^+\bar{\nu}\nu$  [8] and  $K_L \rightarrow \pi^0\bar{\nu}\nu$  [9] are precisely measured. The corre-

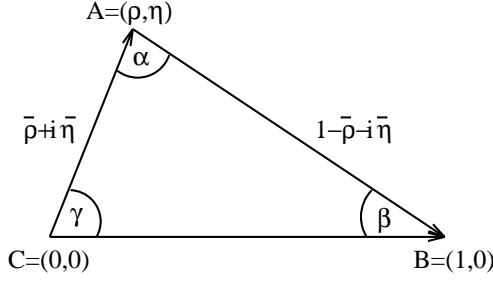


Figure 4. The unitarity triangle. CP-violating observables are usually expressed in terms of its height  $\bar{\eta}$  or one of its angles. The lengths of its sides can be determined from CP-conserving quantities.

sponding phenomenology is condensed into the unitarity triangle depicted in Fig. 4. Its apex  $(\bar{\rho}, \bar{\eta})$  is defined by

$$\bar{\rho} + i\bar{\eta} = -\frac{V_{ud}V_{ub}^*}{V_{cd}V_{cb}^*}, \quad \text{and} \quad \gamma = \arctan\left(\frac{\bar{\eta}}{\bar{\rho}}\right).$$

In addition to  $\bar{\rho}$  and  $\bar{\eta}$  one needs two more quantities to parameterize the CKM matrix,  $\lambda \simeq |V_{us}| = 0.22$  and  $A = |V_{cb}|/\lambda^2 = 0.80 \pm 0.05$ . The Wolfenstein parameterization [10] is an expansion of the CKM matrix in terms of  $\lambda$  to the third order. In CP studies higher orders in  $\lambda$  must be included [11]. In Kaon physics CP-violating quantities are conveniently expressed in terms of

$$\text{Im } \lambda_t = -\text{Im } \lambda_c, \quad \text{where} \quad \lambda_i = V_{is}^* V_{id}. \quad (6)$$

$\lambda_t$  is the CKM factor of the penguin diagrams in Fig. 2 and  $\epsilon'$  is proportional to  $\text{Im } \lambda_t$ . Useful relations are

$$\text{Im } \lambda_t \simeq |V_{cb}||V_{ub}|\sin\gamma \simeq A^2\lambda^5\bar{\eta} \simeq J_{CP}/\lambda \quad (7)$$

Here “ $\simeq$ ” means equal up to corrections of order  $\lambda^2$  or smaller.  $J_{CP}$  is the Jarlskog invariant of CP-violation.  $\bar{\rho}$  and  $\bar{\eta}$  are best suited for the phenomenology of CP-violation in B-physics, yet in Kaon physics CP-violation stems from loop-induced  $s \rightarrow d$  transitions and  $\text{Im } \lambda_t$  is the natural parameter here. Using  $\bar{\eta}$  instead artificially introduces high powers of  $\lambda$  and  $A$  and the associated uncertainties into the problem, see (7). We will also encounter

$$\text{Re } \lambda_t \simeq -(1 - \bar{\rho}) A^2 \lambda^5, \quad \text{Re } \lambda_c \simeq -\lambda. \quad (8)$$

Next we cast (5) into the form

$$\frac{\epsilon'}{\epsilon} = \text{Im } \lambda_t \frac{G_F \omega}{2 |\epsilon| \text{Re } A_0} \left[ \Pi_0 - \frac{1}{\omega} \Pi_2 \right]. \quad (9)$$

Here  $G_F$  is the Fermi constant.  $A_0$  and  $A_2$  are contained in

$$\begin{aligned} \Pi_0 &= \sum_{i=3}^{10} y_i \langle Q_i \rangle_0 (1 - \Omega) \\ &\approx y_6 \langle Q_6 \rangle_0 (1 - \Omega) \\ \Pi_2 &= \sum_{i=7}^{10} y_i \langle Q_i \rangle_2 \approx y_8 \langle Q_8 \rangle_2. \end{aligned} \quad (10)$$

In (10) an operator product expansion has been performed to separate short and long distance physics. The short distance physics is contained in the Wilson coefficients  $y_i$ . The heavy masses of the top quark and the W-boson propagating in the loop diagrams of Fig. 2 enter these coefficients. The  $y_i$  can be reliably calculated in perturbation theory, the state of the art are calculations up to the next-to-leading order in renormalization group improved perturbation theory [12]. Potential new physics contributions enter (10) through extra contributions to the  $y_i$ 's. The long distance physics is non-perturbative and more difficult to calculate. It is contained in the hadronic matrix elements of local four-quark operators  $Q_i$ :

$$\langle Q_i \rangle_I = \langle (\pi\pi)_I | Q_i | K \rangle$$

This notation implicitly excludes the strong hadronic phases, which are factored out of  $A_{0,2}$  in (2), so that the  $\langle Q_i \rangle_I$ 's are real.<sup>2</sup> The strong phases stem solely from elastic  $\pi\pi$  final state rescattering [13]. The 10 operators involved in (10) are

$$\begin{aligned} Q_1 &= (\bar{s}_\alpha u_\beta)_{V-A} (\bar{u}_\beta d_\alpha)_{V-A}, \\ Q_2 &= (\bar{s}u)_{V-A} (\bar{u}d)_{V-A}, \\ Q_{3,5} &= (\bar{s}d)_{V-A} \sum_q (\bar{q}q)_{V\mp A}, \\ Q_{4,6} &= (\bar{s}_\alpha d_\beta)_{V-A} \sum_q (\bar{q}_\beta q_\alpha)_{V\mp A}, \\ Q_{7,9} &= \frac{3}{2} (\bar{s}d)_{V-A} \sum_q e_q (\bar{q}q)_{V\pm A}, \\ Q_{8,10} &= \frac{3}{2} (\bar{s}_\alpha d_\beta)_{V-A} \sum_q e_q (\bar{q}_\beta q_\alpha)_{V\pm A}. \end{aligned} \quad (11)$$

Here  $\alpha, \beta$  are colour indices,  $e_q$  is the quark electric charge and  $(\bar{q}q)_{V\pm A}$  is shorthand for  $\gamma_\nu (1 \pm \gamma_5)$ . Finally isospin breaking from the quark masses ( $m_u \neq$

<sup>2</sup>In [14] the strong phases are included in the definition of  $\langle Q_i \rangle_I$ .

$m_d$ ) is parameterized by  $\Omega$  in (10). The dominant contribution to  $\Pi_0$  in (10) comes from the QCD-penguin operator  $Q_6$  generated by the first diagram of Fig. 2. Likewise  $\Pi_2$  is dominated by the Z-penguins in Fig. 2, which generate  $Q_8$ . Graphically one can obtain the operators in (11) by contracting the corresponding Feynman diagrams to a point.

## 2. Hadronic matrix elements

Here we focus on the dominant operators  $Q_6$  and  $Q_8$  in (10). Their hadronic matrix elements are commonly parameterized in terms of bag factors  $B_6^{(1/2)}$  and  $B_8^{(3/2)}$ :

$$\begin{aligned}\langle Q_6 \rangle_0 &= -4\sqrt{\frac{3}{2}} \left( \frac{m_K^2}{m_s(\mu) + m_d(\mu)} \right)^2 \cdot \\ &\quad (F_K - F_\pi) B_6^{(1/2)}(\mu) \\ \langle Q_8 \rangle_2 &= \sqrt{3} F_\pi \left[ \left( \frac{m_K^2}{m_s(\mu) + m_d(\mu)} \right)^2 \right. \\ &\quad \left. - \frac{1}{6} (m_K^2 - m_\pi^2) \right] B_8^{(3/2)}(\mu).\end{aligned}\quad (12)$$

Here  $m_K, m_\pi, F_K = 160 \text{ MeV}$  and  $F_\pi = 132 \text{ MeV}$  are the masses and decay constants of Kaon and Pion. The renormalization scheme and scale  $\mu$  of the quark masses  $m_s$  and  $m_d$  and the bag factors  $B_6^{(1/2)}, B_8^{(3/2)}$  are defined by the scheme and scale chosen for the operators  $Q_6$  and  $Q_8$ . The vacuum insertion approximation corresponds to  $B_6^{(1/2)} = B_8^{(3/2)} = 1$ .  $\mu$  is chosen to be a scale of order 1 GeV, high enough for QCD perturbation theory to be trusted and low enough for non-perturbative methods to work.

Physical observables like  $\epsilon'$  do not depend on the renormalization scheme and scale. Hence ideally the dependence on the unphysical scale  $\mu$  and the renormalization scheme cancels between the hadronic matrix elements in (12) and the Wilson coefficients  $y_6(\mu)$  and  $y_8(\mu)$  multiplying them in (10). This cancellation indeed occurs in those non-perturbative methods, which use the same degrees of freedom as the perturbative calculation (quarks and gluons) and allow for a matching calculation between the short distance physics contained in the  $y_i$ 's and the long-distance physics residing in the operator matrix elements in

(12). The only known method with this feature is lattice gauge theory. In other methods the remaining dependence on the scheme and scale can be used to estimate the ‘theoretical uncertainty’ of the calculation.

I want to stress here that there is no shortcut to solve this problem: The operator product expansion lumps the physics from all scales larger than  $\mu$  into the Wilson coefficients, while the matrix elements comprise the dynamics associated with scales smaller than  $\mu$ . This enforces heavy mass scales like the top mass to enter the  $y_i$ 's rather than the  $\langle Q_i \rangle$ 's, but it still leaves the freedom to assign any constant factor either to the coefficients or to the matrix elements. Changing the scale  $\mu$  or the scheme chosen to calculate the  $y_i$ 's shuffles such constant factors from the Wilson coefficients to the matrix elements. The quality of the scheme and scale cancellations between coefficients and hadronic matrix elements therefore measures how smoothly the hadronic method chosen to calculate the  $\langle Q_i \rangle$ 's merges into perturbative QCD at the scale  $\mu = \mathcal{O}(1 \text{ GeV})$ . In the literature one can find attempts to cancel this ambiguity in an ad hoc way by adding the perturbatively calculated matrix element to the Wilson coefficients. This formally cancels the scale and scheme dependence of the latter, but introduces the dependence on the infrared regulator instead, which is just another unphysical parameter.

It is important to note that the dominant  $\mu$  dependence of  $Q_6$  and  $Q_8$  in (12) is reproduced by the  $\mu$  dependence of the quark masses. Hence  $B_6^{(1/2)}$  and  $B_8^{(3/2)}$  depend only very weakly on  $\mu$ , so that I omit the reference to  $\mu$  in the following.

Next I summarize the three standard methods to calculate the hadronic parameters  $B_i$ :

**Lattice gauge theory** solves non-perturbative QCD on a discrete spacetime lattice. It controls the scheme and scale dependence of the Wilson coefficients exactly. At present the  $B$ -parameters are calculated in the quenched approximation, i.e. without dynamical fermions. The error caused by this cannot be reliably estimated. Further present calculations determine  $\langle \pi | Q_i | K \rangle$  and  $\langle 0 | Q_i | K \rangle$  on the lattice and relate the result to  $\langle (\pi\pi)_I | Q_i | K \rangle$  using lowest order chiral perturbation theory, thereby introducing additional model dependence. Finally not all systematic errors associated with the discretization of QCD are fully understood yet. Recent lattice results for  $B_8^{(3/2)}$

in the  $\overline{\text{MS}}$  NDR scheme are

$$B_8^{(3/2)} = \begin{cases} 0.77(4)(4) [18] \\ 0.81(3)(3) [19] \\ 0.82(2) [20] \\ 1.03(3) \text{ (non-pert. matching) [20].} \end{cases} \quad (13)$$

The calculation of  $I = 0$  amplitudes is more difficult. A recent calculation of  $B_6^{(1/2)}$  [21] using the new method of domain wall fermions has found a negative  $B_6^{(1/2)}$ , which sharply contradicts the result obtained by other methods and is hardly compatible with experiment even in the presence of new physics [22].

The  $1/N_c$  **expansion** is a rigorous QCD-based method, too. The expansion parameter is the inverse number of colours,  $1/N_c = 1/3$ . The leading order corresponding to  $N_c = \infty$  consists of all planar QCD Feynman diagrams [23]. These diagrams correspond to tree-level diagrams in an effective meson theory, which is based on a chiral lagrangian  $\chi\mathcal{L}$  [24]. Likewise  $1/N_c$  corrections correspond to one-loop diagrams in the meson theory. The loop integrals are calculated with an explicit cutoff  $\Lambda$ , which separates the low energy hadronic region calculated from  $\chi\mathcal{L}$  from the high energy perturbative region of QCD. One can show that  $\Lambda$  appearing in the matrix elements and  $\mu$  contained in the Wilson coefficients are proportional to each other, usually they are taken to be equal. Present calculations yield a quadratic dependence of the matrix elements on  $\Lambda$ , which is expected to turn into the correct logarithmic behaviour of the coefficients once vector mesons are included in the calculation. The scale and scheme dependence of the  $y_i$ 's are exactly cancelled for  $N_c = \infty$  and are qualitatively under control at order  $1/N_c$ . A complete control of the scheme dependence at this order is expected to be possible [25]. In the large- $N_c$  limit one has  $B_6^{(1/2)} = B_8^{(3/2)} = 1$ . Recently  $p^0/N_c$  and  $p^2$  corrections to  $B_6^{(1/2)}$  and  $B_8^{(3/2)}$  in the combined  $1/N_c$  and chiral expansion have been calculated [26]. The predicted ranges for the parameters are

$$0.42 \leq B_8^{(3/2)} \leq 0.64, \quad 0.72 \leq B_6^{(1/2)} \leq 1.30 \quad (14)$$

showing that the corrections to the large  $N_c$  limit are indeed reasonably small, as expected in [24,15,16]. The situation is different in the case of  $B_1^{(1/2)}$  and  $B_2^{(1/2)}$ , which receive anomalously large  $1/N_c$  corrections in qualitative phenomenological agreement

with the large observed value of  $\text{Re } A_0$ . It is common practice to extract the  $B$ -parameters of the subdominant operators in (10) from the experimental values of  $\text{Re } A_0$  and  $\text{Re } A_2$  [15].

The **chiral quark model** [27,28] calculates all  $B$ -parameters in terms of three model parameters, which are determined from  $\text{Re } A_0$  and  $\text{Re } A_2$ . It includes chiral corrections up to  $\mathcal{O}(p^4)$ . The chiral quark model shows a qualitative control of the scale dependence. As in any other model, it is difficult to judge systematic errors of the chiral quark model. My presentation of this model is brief here, because it is covered in some detail in Fabbrichesi's talk [14]. In the  $\overline{\text{MS}}$  HV scheme the predictions for the  $B$ -parameters read:

$$0.75 \leq B_8^{(3/2)} \leq 0.94 \quad 1.1 \leq B_6^{(1/2)} \leq 1.9. \quad (15)$$

### 3. Phenomenology

The Standard Model prediction for  $\epsilon'/\epsilon$  can be summarized in the handy approximate formula [29]:

$$\frac{\epsilon'}{\epsilon} = 21 \cdot 10^{-4} \frac{\text{Im } \lambda_t}{1.7 \cdot 10^{-4}} \left[ \frac{100 \text{ MeV}}{m_s(2 \text{ GeV})} \right]^2 \cdot \left[ B_6^{(1/2)} \frac{1 - \Omega}{0.8} - 0.5 B_8^{(3/2)} \right] \frac{\Lambda_{\overline{\text{MS}}}}{340 \text{ MeV}}. \quad (16)$$

Here  $\Lambda_{\overline{\text{MS}}}$  is the fundamental scale parameter of QCD [30].  $\Lambda_{\overline{\text{MS}}} = 340 \text{ MeV}$  corresponds to  $\alpha_s(M_Z) = 0.119$ .  $\text{Im } \lambda_t$  must be determined from a standard analysis of the unitarity triangle using  $\epsilon$ ,  $|V_{cb}|$ ,  $|V_{ub}|$  and the mass differences  $\Delta m_{d,s}$  of  $B_{d,s}$  mesons. The constraint from  $\epsilon$  in (4) on  $\text{Im } \lambda_t$  reads

$$6.0 \cdot 10^{-8} = \hat{B}_K \text{Im } \lambda_t [\text{Re } \lambda_c [\eta_1 S_{cc} - \eta_3 S_{ct}] - \text{Re } \lambda_t \eta_2 S_{tt}]. \quad (17)$$

Here the result of the box diagram of Fig. 1 is contained in  $S_{cc} = x_c$ ,  $S_{ct} = x_c(0.6 - \log x_c)$  and  $S_{tt} = 2.5$  with  $x_c = m_c^2/M_W^2$  containing the charm quark mass  $m_c \approx 1.3 \text{ GeV}$  in the  $\overline{\text{MS}}$  scheme and the W-boson mass. The well-measured top quark mass has entered the numerical constants 0.6 and 2.5 here.  $\eta_1 = 1.4 \pm 0.2$ ,  $\eta_2 = 0.57 \pm 0.01$  and  $\eta_3 = 0.47 \pm 0.04$  are QCD correction factors [31].  $\hat{B}_K$  in (17) parameterizes the hadronic matrix element of  $\Delta S = 2$  operator generated by the box diagram in Fig. 1. The analyses of the unitarity triangle [31,29] yield:

$$1.0 \cdot 10^{-4} \leq \text{Im } \lambda_t \leq 1.7 \cdot 10^{-4}. \quad (18)$$

The choice of a certain method to calculate the hadronic parameters affects both the phenomenology of  $\epsilon$  in (17) and of  $\epsilon'/\epsilon$  in (16). Thus it correlates  $\text{Im } \lambda_t$  in (16) with  $B_6^{(1/2)}$  and  $B_8^{(3/2)}$ . For example the chiral quark model [27] predicts a higher value for  $\hat{B}_K$  than lattice or  $1/N_c$  calculations. Therefore one extracts a smaller value for  $\text{Im } \lambda_t$  than in (18), where the results of the latter two methods have been used. It must be stressed, however, that the experimental upper limit in (18) stems solely from the upper bounds on  $|V_{ub}|$  and  $|V_{cb}|$ .  $\epsilon_K$  has no influence on the upper limit of  $\text{Im } \lambda_t$ , which is obtained by setting  $\sin \gamma = 1$  in (7).

The strong dependence of  $\epsilon'/\epsilon$  in (16) on  $m_s$  is another big source of uncertainty in the prediction of  $\epsilon'/\epsilon$ . QCD sum rule calculations favour the range [32]

$$m_s(2 \text{ GeV}) = 124 \pm 22 \text{ MeV}. \quad (19)$$

There are now three quenched lattice calculations which control all systematic errors [33]. They are nicely consistent with each other and predict

$$m_s(2 \text{ GeV}) = 103 \pm 10 \text{ MeV}. \quad (20)$$

Further the CP-PACS collaboration [34] has reported the result of an unquenched calculation yielding  $m_s(2 \text{ GeV}) = 84 \pm 7 \text{ MeV}$ . The determination of the strange quark mass from Cabibbo suppressed  $\tau$  decays has been recently clarified by Pich and Prades, who extract

$$m_s(2 \text{ GeV}) = 114 \pm 23 \text{ MeV} \quad (21)$$

from ALEPH data [35].

Finally  $\Omega = 0.25 \pm 0.08$  [36] completes the list of the input parameters of  $\epsilon'/\epsilon$ . From (16) one notes that the  $\Delta I = 1/2$  and  $\Delta I = 3/2$  contributions tend to cancel each other, which increases the uncertainty of the prediction.  $B_6^{(1/2)}$  and  $B_8^{(3/2)}$  enter (16) essentially in the combination  $2B_6^{(1/2)} - B_8^{(3/2)}$ . It is now easy to see from (16) that it is difficult to fit the high measured value in (1) with the  $B$ -parameters in (13) and (14). A recent detailed analysis [29] found

$$\frac{\epsilon'}{\epsilon} = \left(7.7_{-3.5}^{+6.0}\right) \cdot 10^{-4}, \quad (22)$$

substantially below the experimental result. On the other hand it is possible to reach the value in (1), if simultaneously  $2B_6^{(1/2)} - B_8^{(3/2)}$  is large and  $m_s$  is

small [29,37]. In [37] an upper bound on  $m_s$  has been derived from the requirement that  $\epsilon'/\epsilon \geq 20 \cdot 10^{-4}$  corresponding to the  $2\sigma$  bound of the KTeV measurement [3]. If  $2B_6^{(1/2)} - B_8^{(3/2)} \leq 2.0$  suggested by (13) and (14), then

$$m_s(2 \text{ GeV}) \leq 110 \text{ MeV}. \quad (23)$$

This is in agreement with (20) and (21), but not with all sum rule results represented by the range in (19). As discussed at this conference, especially values for  $m_s(2 \text{ GeV})$  below 100 MeV are in serious conflict with QCD sum rule calculations. Such low values would imply that the breakdown of the perturbative calculations of the relevant spectral functions sets in at a much higher scale than commonly expected.

The chiral quark model allows for a larger range for  $2B_6^{(1/2)} - B_8^{(3/2)}$  in (15). It predicts [28]

$$\frac{\epsilon'}{\epsilon} = \left(17_{-10}^{+14}\right) \cdot 10^{-4}, \quad (24)$$

in better agreement with the data in (1). The difference between (24) and (22) stems not only from the different ranges for the  $B$ -parameters in (15) and (14) but also from a different treatment of the final state phases: None of the methods described in sect. 2 predicts the strong phases  $\delta_{0,2}$  correctly. Lattice calculations cannot do this, because they are performed with Euclidean time. The other two methods find  $\delta_0$  much smaller than the experimental value  $\delta_0^{exp} = 37^\circ$ . This leads to some ambiguity in the prediction for  $\epsilon'/\epsilon$ , because one can either identify the magnitude or the real part of the calculated  $\langle Q_6 \rangle_0 \exp(i\delta_0^{calc})$  with the desired true  $\langle Q_6 \rangle_0 \exp(i\delta_0^{exp})$ . The former identification has been chosen in [24,15,16] with the result quoted in (22), while the Trieste group [14,27,28] has used the real part in their prediction of (24). One can implement the Trieste method into the  $1/N_c$  result by rescaling the range for  $B_6^{(1/2)}$  in (14) by a factor of  $1/\cos(\delta_0^{exp}) = 1.25$  to  $0.9 \leq B_6^{(1/2)} \leq 1.6$ . This increases the range for  $\epsilon'/\epsilon$  in (22) and relaxes the upper bound on  $m_s(2 \text{ GeV})$  in (23) to 125 MeV. Hence a part of the discrepancy between (22) and (24) stems from the treatment of the strong phases and has nothing to do with the different treatment of the strong dynamics.

Do we need  $m_s$  at all to predict  $\epsilon'/\epsilon$ ? The strange quark mass enters the hadronic matrix elements in

(12), because they are normalized to their value in the vacuum insertion approximation. In the distant future lattice calculations might directly compute the matrix elements in (12) proportional to  $B_i/m_s^2$  rather than  $m_s$  and the  $B_i$ 's separately. Yet it should be stressed that present lattice results summarized in (13) stem from calculations of the B-parameter  $B_8^{(3/2)}$  rather than the full matrix element. The importance of  $m_s$  for the prediction of  $\epsilon'/\epsilon$  in lattice calculations has been stressed in [38]. Also the  $1/N_c$  expansion naturally introduces the factor  $1/m_s^2$  into (12): In the large- $N_c$  limit the matrix elements of  $Q_6$  and  $Q_8$  reduce to those of density currents  $\bar{s}q_{S+P} = \bar{s}(1 + \gamma_5)q$  and  $\bar{q}d_{S-P}$ . They are related to vector currents by the equation of motion, which introduces  $m_s$  into the result. The B-parameters obtained in the  $1/N_c$  expansion are independent of  $m_s$ . Other methods express matrix elements of (density) $\times$ (density) operators in terms of the quark condensate, which is related to  $m_s$  and  $m_K$  by the PCAC relation. In these methods the parametrization in (12) may be unnatural and the thereby defined B-parameters can exhibit a sizeable dependence on  $m_s$ . E.g. in the chiral quark model  $B_6^{(1/2)}$  is proportional to  $m_s$ .

The second possibility to reproduce (1) is to consider higher values for  $B_6^{(1/2)}$ , as suggested by the chiral quark model in (15). An important feature of the chiral quark model is the proliferation of the  $\Delta I = 1/2$  enhancement present in  $\text{Re } A_0$  (cf. (3)) into  $B_6^{(1/2)}$ . The three parameters of the chiral quark model are determined from the  $\Delta I = 1/2$  rule which thereby feeds into  $B_6^{(1/2)}$ . The enhancement of  $\text{Re } A_0$  originates from penguin contractions of the operators  $Q_1$  and  $Q_2$  [24,29], which involve the same spin and isospin quantum numbers as  $Q_6$ . The fact that the chiral quark model can reproduce (1) more easily could indicate that a  $\Delta I = 1/2$  enhancement is at work in  $B_6^{(1/2)}$  as well [39]. This hypothesis has also been recently stressed by the Dortmund group [40], which found indication of a further enhancement of  $B_6^{(1/2)}$  from a higher order term ( $\mathcal{O}(p^2/N_c)$ ) in the  $1/N_c$  expansion. It is worthwhile to notice that the  $1/N_c$  expansion fails to simultaneously reproduce both  $\text{Re } A_0$  and  $\text{Re } A_2$  [41]. The second reason for the large value of  $\epsilon'/\epsilon$  in (24) is the special treatment of the final state phases as described after (24), which is controversial [29]. It is highly desirable to gain a full dynamical

understanding of both the  $\Delta I = 1/2$  enhancement in  $\text{Re } A_0$  and possibly in  $B_6^{(1/2)}$  and the large final state interaction phase  $\delta_0 = 37^\circ$  causing the discussed ambiguity in  $\epsilon'/\epsilon$ . To this end in [37,42] a resonant enhancement of  $\langle Q_6 \rangle_0$  caused by the  $\sigma = f_0(400 - 1200)$  [43] resonance has been discussed.  $\sigma$  is a broad S-wave  $I = 0$  resonance almost degenerate in mass with the Kaon. In theories based on a chiral lagrangian  $\sigma$  corresponds to resonant  $\pi\pi$  rescattering in the  $I = 0$  channel, an all-order effect depicted in Fig. 5. Unfortunately the progressing lattice calculations will not help to understand such a resonant enhancement of  $B_6^{(1/2)}$ , because they will determine  $\langle \pi | Q_i | K \rangle$  rather than  $\langle (\pi\pi)_0 | Q_i | K \rangle$ ! Even if reliable lattice results for  $\langle \pi | Q_i | K \rangle$  are present, there will still be a sizeable model dependence in the prediction of  $B_6^{(1/2)} \propto \langle (\pi\pi)_0 | Q_i | K \rangle$ .

Finally another source of theoretical uncertainties has been recently suggested [44]: Isospin violations in  $\langle Q_6 \rangle$  resulting from  $m_u \neq m_d$  can substantially enlarge the range  $0.15 \leq \Omega \leq 0.35$  used in [28,29].

#### 4. New physics

Since  $\epsilon'/\epsilon$  is a short distance dominated process, it is sensitive to new physics, which can modify the Wilson coefficients  $y_i$ . The  $y_i$ 's are generated by Feynman diagrams like those in Fig. 2 at some high scale  $\mu$  of the order of  $M_W$  or of the mass of some new particle entering the loop diagrams. The renormalization group evolution down to the scale  $\mu \approx 1 \text{ GeV}$ , at which the matrix elements in (10) are calculated, mixes the coefficients  $y_i$ . Now  $y_6(\mu \approx 1 \text{ GeV})$  is mainly an admixture of the Wilson coefficient of  $Q_2$ , which is generated by tree-level  $W$ -exchange and is therefore hardly affected by new physics. On the other hand  $y_8(\mu \approx 1 \text{ GeV})$  is merely loop-induced and stems mainly from the  $\bar{s}dZ$ -vertex (see Fig. 2). It is therefore sensitive to new physics. If new contributions to  $y_8$  have the opposite sign of the Standard Model contribution,  $\epsilon'/\epsilon$  will be enhanced. Further the chromomagnetic operator

$$Q_{11} = \frac{g_s}{16\pi^2} m_s \bar{s} \sigma^{\mu\nu} T^a (1 - \gamma_5) d G_{\mu\nu}^a. \quad (25)$$

can play a role. In the Standard Model its coefficient equals  $y_{11}(\mu \approx 1 \text{ GeV}) \approx -0.19$  and the impact on  $\epsilon'/\epsilon$  is negligible [27], so that  $y_{11} \langle Q_{11} \rangle_0$  has been

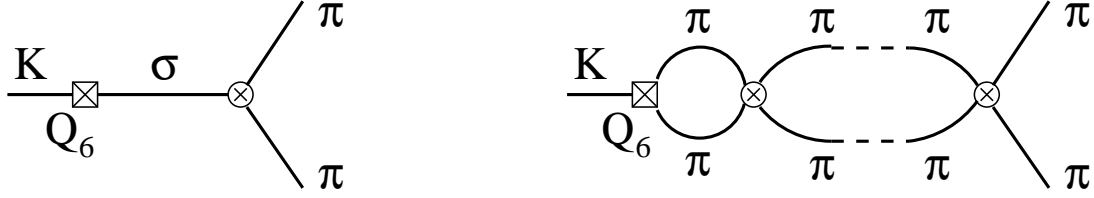


Figure 5. The  $\sigma = f_0(400 - 1200)$  resonance enhances  $\langle (\pi\pi)_0 | Q_i | K \rangle \propto B_6^{(1/2)}$ . It corresponds to resonant  $\pi\pi$  rescattering in the  $I = 0$  channel as depicted by the right diagram. The crossed square denotes the weak interaction mediated by  $Q_6$  and the crossed circles represent strong interaction vertices.

omitted in (10). A model-independent discussion of new contributions to  $y_8$  and  $y_{11}$  has been performed in [37]. An enhancement of the Standard Model result for  $y_{11}$  by a factor of order 500 is necessary for a sizeable impact on  $\epsilon'/\epsilon$ .

The high experimental value in (1) has stimulated new theoretical work on possible new physics contributions to  $\epsilon'/\epsilon$ , mainly in supersymmetric theories. Supersymmetry (SUSY) does not help to understand the puzzles of flavour physics. Moreover, the minimal supersymmetric standard model with the most general soft SUSY-breaking mechanism leads to unacceptably large flavour-changing neutral transitions. Hence additional assumptions on the SUSY-breaking terms are necessary, most commonly flavour-blindness of these terms (“universality”) at some high scale. Yet in these scenarios the impact of SUSY on  $\epsilon'/\epsilon$  is small, and in most of the parameter space  $\epsilon'/\epsilon$  is depleted rather than enhanced [45]. Alternatively one can relax the universality assumption and allow for arbitrary flavour off-diagonal entries in the squark mass matrix. Here one proceeds phenomenologically, encounters all experimental constraints from other flavour-changing processes [46] and finally estimates the maximal impact on  $\epsilon'/\epsilon$  or other processes of interest. In these generic SUSY models, however, the situation for  $\epsilon'/\epsilon$  is different than in scenarios with flavour universality: It is possible to have sizeable contributions to the imaginary parts of the  $\bar{s}dZ$ -vertex affecting  $y_8$  [47] and the chromomagnetic  $\bar{s}d$ -gluon-vertex modifying  $y_{11}$  [48,49] without violating the stringent bounds from Kaon mixing and other flavour-changing processes. Then  $\epsilon'/\epsilon$  can even be dominated by new physics. In [49] an approximate flavour sym-

metry controlling the Yukawa matrix and the SUSY A-matrix has been postulated. Then the small weak  $s \rightarrow d$  transition proportional to  $\text{Im } \lambda_t = \mathcal{O}(\lambda^5)$  in (17) is replaced by a strong transition of order  $\lambda$  producing the necessary enhancement factor. A recent detailed analysis [50] has found an enhancement of  $\epsilon'/\epsilon$  through  $y_{11}$  more likely than through  $y_8$ . Finally in addition a mass splitting between up and down squarks also generates new  $\Delta I = 3/2$  contributions via box diagrams which likewise influence  $\epsilon'/\epsilon$  [51].

## 5. Conclusions and outlook

It is difficult, but possible to accomodate  $\epsilon'/\epsilon \simeq 2 \cdot 10^{-3}$  in the Standard Model. I have discussed the following mechanisms to explain the large measured value in (1):

- 1) Small  $m_s$  as indicated by recent lattice results [33,34].
- 2)  $\Delta I = 1/2$  enhancement of  $B_6^{(1/2)}$  [37,39,40].
- 3) Larger isospin breaking characterized by the parameter  $\Omega$  [44].
- 4) Decrease of the imaginary part of the  $\bar{s}dZ$ -vertex (and thereby of  $y_8$ ) by new physics [47,50].
- 5)  $\mathcal{O}(500)$  enhancement of the chromomagnetic  $\bar{s}d$ -gluon-vertex (and thereby of  $y_{11}$ ) by new physics [48–50].

In the future one can expect improvements in the prediction of  $\epsilon'/\epsilon$  from a better knowledge of  $m_s$  from  $\tau$ -decays [35] and from a better determination of  $\text{Im } \lambda_t$ ,

once the dedicated B- and K-experiments [6–9] will give us a clear picture of the unitarity triangle. On the other hand I do not expect much progress in  $B_6^{(1/2)}$  from lattice calculations, because these calculations will not determine  $\langle (\pi\pi)_0 | Q_i | K \rangle$  directly. Hence the question of new physics in  $\epsilon'/\epsilon$  will stay inconclusive and the corresponding new contributions will more likely be revealed in the measurements [8,9] of rare Kaon decays [47,50].

### Acknowledgements

I thank Matthias Neubert for inviting me to this conference and Stephane Narison and his team for creating the pleasant and stimulating atmosphere. I have enjoyed a lot of fruitful discussions with many colleagues. I am grateful to Andrzej Buras for proof-reading the manuscript.

**COMMENT (M. Knecht, CPT/CNRS Marseille):**  
*I have a comment to A. Pich's comment concerning the dependence of  $\epsilon'/\epsilon$  on the size of the quark condensate. If one does the things correctly within the framework of generalized  $\chi$ PT, one finds that the prediction for  $\epsilon'/\epsilon$  can easily be increased by a factor of 3, taking all other parameters fixed, i.e.  $m_s(2\text{ GeV}) \sim 150\text{ MeV}$ , if the condensate was smaller by a factor of 10.*

### REFERENCES

1. D. BARR ET AL., Phys. Lett. B317 (1993) 233.
2. L.K. GIBBONS ET AL. Phys. Rev. Lett.70 (1993) 1203.
3. A. ALAVI-HARATI ET AL. Phys. Rev. D55 (1999) 22.
4. P. DEBU, CERN seminar, June 18, 1999, <http://www.cern.ch/NA48>.
5. J. H. CHRISTENSON, J. W. CRONIN, V. L. FITCH AND R. TURLAY, Phys. Rev. Lett. 13 (1964) 138; Phys. Rev. 140B (1965) 74.
6. D. BOUTIGNY ET AL., *BaBar technical design report*, SLAC-R-0457. M.T. CHENG ET AL. (BELLE COLLAB.), *A study of CP violation in B meson decays: Technical design report*, BELLE-TDR-3-95.
7. K. PITTS (FOR FERMILAB D0 AND CDF COLLAB.), Proceedings 4th Workshop on Heavy Quarks at Fixed Target (HQ 98), Batavia, USA, 1998. P. KRIZAN ET AL., *HERA-B, an experiment to study CP violation at the HERA proton ring using an internal target*, Nucl. Instrum. Meth. A351 (1994) 111; DAVID WEBSDALE, *LHC-B: A dedicated B physics detector for the LHC*, Nucl. Phys. Proc. Suppl. 50 (1996) 333.
8. P. COOPER ET AL. (CKM COLLAB.), *EOI for measuring  $Br(K^+ \rightarrow \pi^+ \nu \bar{\nu})$  at the Main Injector*, FERMILAB EOI 14, 1996. L.H. CHIANG ET AL., *Proceedings of the AGS-2000 workshop*, ed. L.S. Littenberg and J. Sandweiss, 1 (1996).
9. K. ARISAKA ET AL., *Conceptual design report: Kaons at the Main Injector*, FERMILAB-FN-568, 1991. L.H. CHIANG ET AL. AGS proposal 926 (1996);
10. L. WOLFENSTEIN, Phys. Rev. Lett.51 (1983) 1945.
11. A. J. BURAS, M. E. LAUTENBACHER, G. OSTERMAIER, Phys. Rev. D50 (1994) 3433.
12. A.J. BURAS, M. JAMIN AND M.E. LAUTENBACHER, Nucl. Phys. B370 (1992) 69, Nucl. Phys. B400 (1993) 37, Nucl. Phys. B400 (1993) 75. M. CIUCHINI, E. FRANCO, G. MARTINELLI AND L. REINA, Phys. Lett. B301 (1993) 263, Nucl. Phys. B415 (1994) 403.
13. K.M. WATSON, Phys. Rev. 88 (1952) 1163.
14. M. FABBRICHESI, *Talk at QCD'99, Montpellier, France 1999*, these proceedings and hep-ph/9909224.
15. A.J. BURAS, M. JAMIN AND M.E. LAUTENBACHER, Nucl. Phys. B408 (1993) 209.
16. A.J. BURAS, hep-ph/9806471, to appear in *Probing the Standard Model of Particle Interactions*, ed. F.David and R. Gupta, Elsevier Science B.V, 1999.
17. A.J. BURAS AND L. SILVESTRINI, Nucl. Phys. B546 (1999) 299.
18. G. KILCUP, R. GUPTA, S.R. SHARPE, Phys. Rev. D57 (1998) 1654.
19. R. GUPTA, T. BHATTACHARAYA AND S.R. SHARPE, Phys. Rev. D55 (1997) 4036.
20. L. CONTI, A. DONINI, V. GIMENEZ, G. MARTINELLI, M. TALEVI AND A. VLADIKAS, Phys. Lett. B421 (1998) 273.
21. T. BLUM ET AL., hep-lat/9908025.
22. S. BERTOLINI AND M. FABBRICHESI, hep-ph/9908474.

23. G. 'T HOOFT, Nucl. Phys. B72 (1974) 461.
24. W.A. BARDEEN, A.J. BURAS AND J.-M. GÉRARD, Phys. Lett. B180 (1986) 133, Nucl. Phys. B293 (1987) 787, Phys. Lett. B192 (1987) 138.
25. W.A. BARDEEN, Nucl. Phys. Proc. Suppl. 7A (1989) 149; W.A. BARDEEN *in preparation*.
26. T. HAMBYE, G.O. KÖHLER, E.A. PASCHOS, P.H. SOLDAN AND W.A. BARDEEN, Phys. Rev. D58 (1998) 014017.
27. S. BERTOLINI, M. FABBRICHESI AND J.O. EEG, Nucl. Phys. B449 (1995) 197, Nucl. Phys. B476 (1996) 225. S. BERTOLINI, M. FABBRICHESI, J.O. EEG AND E.I. LASHIN, Nucl. Phys. B514 (1998) 93.
28. S. BERTOLINI, M. FABBRICHESI AND J.O. EEG, hep-ph/9802405.
29. S. BOSCH, A.J. BURAS, M. GORBAHN, S. JÄGER, M. JAMIN, M.E. LAUTENBACHER AND L. SILVESTRINI, hep-ph/9904408. A.J. BURAS, *Talk at KAON'99, Chicago, USA 1999*, hep-ph/9908395.
30. W. A. BARDEEN, A. J. BURAS, D. W. DUKE AND T. MUTA, Phys. Rev. D18 (1978) 3998.
31. A.J. BURAS, M. JAMIN AND P.H. WEISZ, Nucl. Phys. B347 (1990) 491, S. HERRLICH AND U. NIERSTE, Nucl. Phys. B419 (1994) 292, Phys. Rev. D52 (1995) 6505, Nucl. Phys. B476 (1996) 27.
32. K.G. CHETYRKIN, D. PIRJOL AND K. SCHILCHER, Phys. Lett. B404 (1997) 337. P. COLANGELO, F. DE FAZIO, G. NARDULLI AND N. PAVER, Phys. Lett. B408 (1997) 340. M. JAMIN, Nucl. Phys. Proc. Suppl. 64 (1998) 250. S. NARISON, hep-ph/9905264. S. NARISON, *Talk at QCD'99, Montpellier, France 1999*, these proceedings.
33. S. AOKI ET AL. (JLQCD COLLAB.), Phys. Rev. Lett. 82 (1999) 4392. M. GÖCKELER (QCDSF COLLAB.), hep-lat/9908005. J. GARDEN, J. HEITGER, R. SOMMER AND H. WITTIG (ALPHA/UKQCD COLLAB.), hep-lat/9906013.
34. A. ALI KHAN ET AL. (CP-PACS COLLAB.), *Talk given at 17th International Symposium on Lattice Field Theory (LATTICE 99), Pisa, Italy, 1999*.
35. A. PICH AND J. PRADES, hep-ph/9909244. A. PICH, *Talk at QCD'99, Montpellier, France 1999*, these proceedings and hep-ph/9909559.
36. R. BARATE ET AL. (ALEPH COLL.), hep-ex/9903014 and hep-ex/9903015.
37. J.F. DONOGHUE, E. GOLOWICH, B.R. HOLSTEIN AND J. TRAMPETIC, Phys. Lett. B179 (1986) 361. A.J. BURAS AND J.M. GÉRARD, Phys. Lett. B192 (1987) 156. M. LUSIGNOLI, Nucl. Phys. B325 (1989) 33.
38. Y. KEUM, U. NIERSTE AND A.I. SANDA, Phys. Lett. B457 (1999) 157.
39. G. MARTINELLI, Nucl. Phys. Proc. Suppl. 73 (1999) 58.
40. S. BERTOLINI, *Talk at KAON'99, Chicago, USA 1999*, hep-ph/9908268.
41. T. HAMBYE, G.O. KÖHLER, E.A. PASCHOS AND P.H. SOLDAN, hep-ph/9906434.
42. T. HAMBYE, G.O. KÖHLER AND P.H. SOLDAN, hep-ph/9902334.
43. T. MOROZUMI, C.S. LIM AND A.I. SANDA, Phys. Rev. Lett. 65 (1990) 404.
44. K.S. BABU ET AL. (PARTICLE DATA GROUP), Eur. Phys. J. C3 (1998) 1, p. 25.
45. S. GARDNER AND G. VALENCIA, hep-ph/9909202.
46. E. GABRIELLI AND G.F. GIUDICE, Nucl. Phys. B433 (1995) 3.
47. F. GABBIANI, E. GABRIELLI, A. MASIERO AND L. SILVESTRINI, Nucl. Phys. B477 (1996) 321.
48. G. COLANGELO AND G. ISIDORI, JHEP 09 (1998) 009. A.J. BURAS AND L. SILVESTRINI, Nucl. Phys. B546 (1999) 299.
49. S. BERTOLINI, F. BORZUMATI AND A. MASIERO, Nucl. Phys. B294 (1987) 321. A.L. KAGAN, Phys. Rev. D51 (1995) 6196.
50. A. MASIERO AND H. MURAYAMA, hep-ph/9903363.
51. A.J. BURAS, G. COLANGELO, G. ISIDORI, A. ROMANINO AND L. SILVESTRINI, hep-ph/9908371.
52. A.L. KAGAN AND M. NEUBERT, hep-ph/9908404.